Biophysical Letter

Molecular Flow Quantified beyond the Diffraction Limit by Spatiotemporal Image Correlation of Structured Illumination Microscopy Data

George W. Ashdown,[1] Andrew Cope,[2] Paul W. Wiseman,[3] and Dylan M. Owen[1,*]
[1]Department of Physics and Randall Division of Cell and Molecular Biophysics and [2]Academic Department of Rheumatology, Centre for Molecular and Cellular Biology of Inflammation, Division of Immunology, Infection and Inflammatory Disease, King's College London, London, United Kingdom; and [3]Departments of Chemistry and Physics, McGill University, Montreal, Quebec, Canada

ABSTRACT We combine total internal reflection fluorescence structured illumination microscopy with spatiotemporal image correlation spectroscopy to quantify the flow velocities and directionality of filamentous-actin at the T cell immunological synapse. These techniques demonstrate it is possible to image retrograde flow of filamentous-actin at superresolution and provide flow quantification in the form of velocity histograms and flow vector maps. The flow was found to be retrograde and radially directed throughout the periphery of T-cells during synapse formation.

Received for publication 31 July 2014 and in final form 16 September 2014.

*Correspondence: dylan.owen@kcl.ac.uk

Many biological processes are now being visualized with the use of superresolution fluorescence microscopy techniques. However, localization-based techniques primarily rely on fixed or slow moving samples to permit the collection of structural information. The 10-fold gains in resolution afforded by these superresolution techniques are usually possible through sacrificing the factors that originally made microscopy such a powerful tool: the ability to image live cells. In the case of stimulated emission depletion imaging, the scanning approach associated with this technique may fail to detect faster molecular events when imaging whole cellular regions.

Structured illumination microscopy (SIM) is an alternative to these methods (1). It increases the resolution of conventional fluorescence microscopy twofold; it has the advantage of using a wide-field system, providing fast acquisition speeds of whole cells with relatively low laser powers; and it is compatible with standard fluorophores. By using a physical grating to produce interference patterns from a laser, periodic illumination is created. This patterned illumination causes information from higher spatial frequencies to be downmodulated (i.e., shifted) into the optical transfer function (support region) of the lens, resulting in higher-resolution spatial information being captured than is ordinarily obtainable.

To quantify the directional motion of intracellular molecules, spatiotemporal image correlation spectroscopy (STICS (2)) was applied. Using spatial image correlation in time, STICS measures the similarity of pixels with those surrounding in lagging frames via a correlation function. The correlation function provides information on both flow velocities and directionality, while discounting static structures through the immobile object filter, achieved by subtracting a moving average of pixel intensities.

The formation of an immunological synapse between T cells and antigen-presenting cells is a process requiring many dynamic (3) and subdiffraction-limited clustering events (4–6) to take place. The polymerization of actin is important for the spreading of cells over their target antigen-presenting cells (7), as well as cell mobility and migration (8). Retrograde flow of densely meshed cortical actin is observed at the basal membrane of synapse-forming T cells, where it may have a role in the corralling and clustering of signaling molecules at the plasma membrane (9), as well as at the leading edge of migrating cells (10). Filamentous actin is an extremely dynamic (7), densely packed, and thin (7-nm) structure (11,12).

Here, we perform STICS on SIM data acquired on a total internal reflection fluorescence (TIRF) microscope system, which generated an evanescent field of 75-nm depth for excitation. To our knowledge, this is the first demonstration of an image correlation approach to quantify molecular dynamics on subresolution length scales using wide-field microscopy. To demonstrate the technique, we analyze two-dimensional actin flows in $CD4^+$ T cells during immunological synapse formation, performed after cross-linking of antigen T cell receptors on a coverslip coated with specific antibodies.

Fig. 1 *a* shows a schematic of the TIRF SIM setup. Excitation light (488 nm) passes through a polarizing module and then a phase-grating block, producing diffracted beams. These are then passed through a diffraction filter module to isolate the -1 and $+1$ order laser beams. These first-order

Editor: David Wolf.

http://dx.doi.org/10.1016/j.bpj.2014.09.018

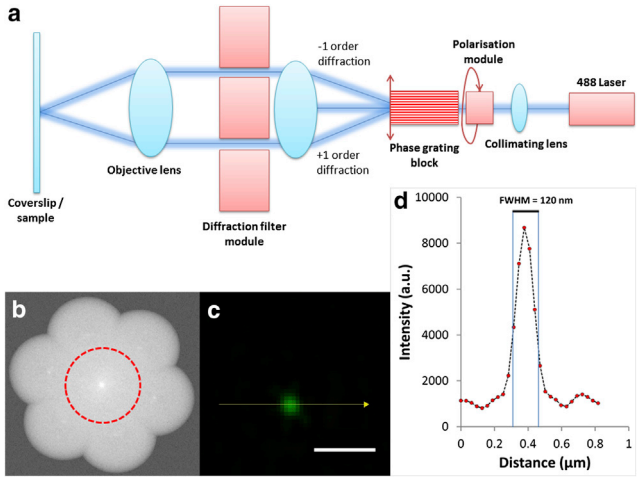

FIGURE 1 (***a***) **Schematic of the TIRF SIM setup. (*b*) Demonstration of the doubling of spatial resolution of collected frequencies through a Fourier transform (*superimposed red circle* demonstrating regular spatial frequency limits). (*c*) SIM reconstructed image of 100-nm bead (scale bar 0.5 μm). (*d*) (*Plotted line*) Bead showing full width at half-maximum of 120 nm.**

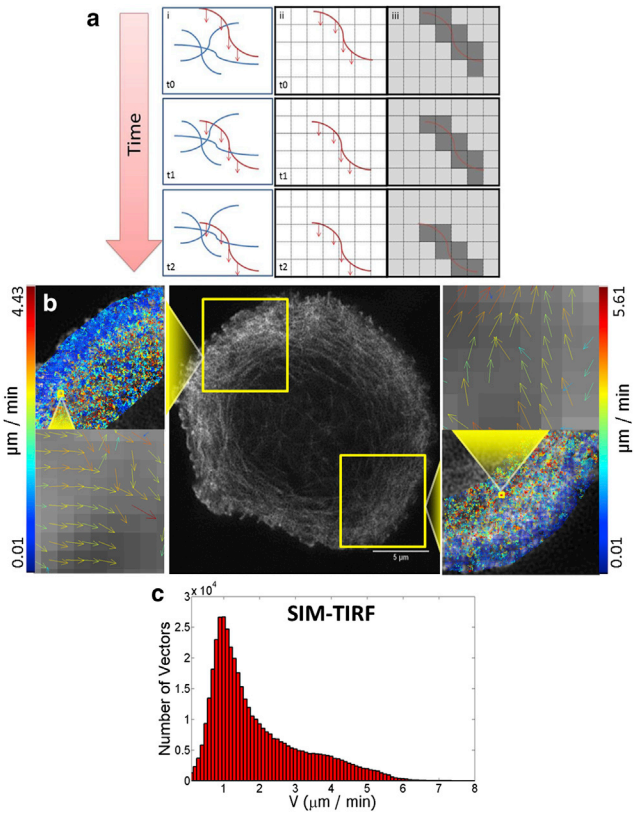

FIGURE 2 (***a***) **STICS analysis, performed by isolating mobile from immobile structures through a moving average filter (*i*) and binning a subset of pixels into blocks of superpixels (*ii*); the STICS software correlates spatial fluorescence fluctuations through time (*iii*). The code then outputs vector maps showing directionality and flow velocities. (*b*) TIRF SIM image of actin flow in a T cell 5 min after contact with a stimulatory coverslip. (*Zoomed regions*) Retrograde actin flow at the synapse periphery. (*c*) Histograms showing flow speed statistics of vectors from T-cell synapses ($n = 7$).**

laser beams are angled through the objective to produce total internal reflection conditions at the glass-water interface. The two evanescent waves interfere at the sample, producing structured illumination. The setup then produces lateral and rotational shifts through three orientations, producing nine raw images containing higher spatial frequencies than can normally be acquired by an objective using standard light microscopy. Fig. 1 *b* demonstrates the increased resolution obtained from TIRF SIM. Shown are the collected Fourier frequencies compared to those of a conventional microscope (*dotted red line*). Resolution was also measured using sparse 100-nm diameter fluorescent beads. Fig. 1 *c* shows a magnified image of these beads from which a line profile was obtained (*yellow arrow*). The full width at half-maximum of this profile (Fig. 1 *d*) gives a lateral resolution for the system of 120 nm.

We then applied STICS analysis to quantify actin flow in T cell synapses acquired using TIRF SIM (Fig. 2). Fig. 2 *a* shows a schematic of the STICS analysis. From the raw data, immobile objects are first filtered by subtracting a moving average of the pixel values. Vector maps were obtained from correlation analysis of the time-series as previously published in Hebert et al. (2) and Brown et al. (13). Fig. 2 *b* shows a reconstructed TIRF SIM image of a mature T cell immunological synapse, representative of a time-point derived from the time series acquired at 1.28 fps (see Movie S1 in the Supporting Material). From this reconstructed image, two representative regions have been selected. In these regions, pseudo-colored actin flow vectors are overlaid onto the fluorescence intensity image. These range in magnitude from 0.01 μm/min (*blue*) to 5.61 μm/min (*red*). It can be observed that all flow vectors are directed radially toward the synapse center. A histogram of this flow is shown in Fig. 2 *c*. The histogram shows a peak retrograde flow velocity of 1.91 $\pm$ 1.27 μm/min. These data are representative of $n = 7$ T-cell synapses imaged by TIRF SIM.

METHOD

Jurkat T cells were cultured in RPMI 1640 medium supplemented with 10% FCS and 1% penicillin and streptomycin, at 37°C in a 5% CO_2 atmosphere. Cells were transfected with LifeAct-EGFP by electroporation 24 h before imaging. T-cells were resuspended at 37°C in 1× HBSS, supplemented with 20 mM HEPES and stimulated to generate immunological synapses after stimulation with specific antibodies (αCD3 and αCD28; BioLegend, San Diego, CA and BD Bioscience, Franklin Lakes, NJ) immobilized on No. 1.0 coverslip-bottomed dishes (Labtek, Brendale, Queensland, Australia). Synapses were allowed to mature for 5–10 min at 37°C before imaging.

TIRF SIM imaging was carried out on an N-SIM system (Nikon, Tokyo, Japan) with a 100× 1.49 NA oil-immersion objective using a 488-nm excitation laser to image at 1.28 fps for 3–5 min. All cells were imaged at 37°C. SIM images were reconstructed in the ANALYZE software (Nikon) at a pixel resolution of 30 nm, with illumination modulation contrast and high-resolution noise suppression both set to 1.

STICS analysis of the first 50 frames was performed using the software MATLAB (Ver. 0.29; The MathWorks, Natick, MA; http://wiseman-group.mcgill.ca/). Immobile objects were filtered by subtracting an average frame of 21 frames through time, from each subregion image. Vector maps were generated by binning 8 × 8 pixels into a superpixel. These binned pixels were shifted by 1 pixel to generate the next vector. Maximum lag times were set at 20 images.

CONCLUSION

Superresolution fluorescence microscopy is becoming an increasingly popular tool for biological research, but not all techniques are fully compatible with live-cell imaging and measurement of dynamics. Here, we have demonstrated that TIRF SIM imaging can be combined with STICS analysis to quantify molecular dynamics on subresolution length scales in live cells. For SIM data, an image resolution of 120 nm was achieved, which allowed the generation of flow vector maps rendered at a grid spacing of 30 nm with each vector generated using data from a 240-nm-square area. We applied this methodology to the analysis of actin flow at the T cell immunological synapse formed against an activating, anti-body-coated coverslip.

Using our approach, we show that cortical filamentous actin at the synapse periphery (i.e., dSMAC) flows in a retrograde fashion toward the cell center (i.e., cSMAC) even in mature synapses. This is consistent with previous analysis of actin flows via kymographs and conventional resolution microscopy (7,14) that also showed retrograde flow, but at reduced spatial resolution. Our analysis showed that the velocity of the mobile fraction of actin was at ~0.5–4 μm per min, again, consistent with previous data.

Limitations of this technique include the TIRF illumination, which, due to the evanescent wave depth, requires a flat sample close to the coverslip. This is required inasmuch as the STICS analysis assumes a two-dimensional molecular flow. Reconstructed SIM images require nine raw images (frame rates limited to $\approx$ 1 s, based on 50-ms exposure times).

The noninvasive nature and live-cell compatibility of fluorescence microscopy is part of what made the technique so widespread. These advantages are not available with all superresolution imaging techniques. We believe that the combination of live-cell TIRF SIM and image correlation approaches will be a powerful tool for quantifying molecular flow on subresolution length scales.

SUPPORTING MATERIAL

One movie is available at http://www.biophysj.org/biophysj/supplemental/S0006-3495(14)00957-6.

ACKNOWLEDGMENTS

We acknowledge the Nikon Imaging Centre at King's College London.

D.M.O. acknowledges European Research Council grant No. 337187 and the Marie-Curie Career Integration Grant No. 334303. P.W.W. acknowledges the Natural Sciences and Engineering Research Council of Canada's Discovery Grant program.

REFERENCES and FOOTNOTES

1. Gustafsson, M. G. 2000. Surpassing the lateral resolution limit by a factor of two using structured illumination microscopy. *J. Microsc.* 198:82–87.
2. Hebert, B., S. Costantino, and P. W. Wiseman. 2005. Spatiotemporal image correlation spectroscopy (STICS) theory, verification, and application to protein velocity mapping in living CHO cells. *Biophys. J.* 88:3601–3614.
3. Campi, G., R. Varma, and M. L. Dustin. 2005. Actin and agonist MHC-peptide complex-dependent T cell receptor microclusters as scaffolds for signaling. *J. Exp. Med.* 202:1031–1036.
4. Sherman, E., V. Barr, and L. E. Samelson. 2013. Super-resolution characterization of TCR-dependent signaling clusters. *Immunol. Rev.* 251:21–35.
5. Lillemeier, B. F., M. A. Mörtelmaier, …, M. M. Davis. 2010. TCR and Lat are expressed on separate protein islands on T cell membranes and concatenate during activation. *Nat. Immunol.* 11:90–96.
6. van der Merwe, P. A., P. D. Dunne, …, S. J. Davis. 2010. Taking T cells beyond the diffraction limit. *Nat. Immunol.* 11:51–52.
7. Babich, A., S. Li, …, J. K. Burkhardt. 2012. F-actin polymerization and retrograde flow drive sustained PLCγ1 signaling during T cell activation. *J. Cell Biol.* 197:775–787.
8. Mogilner, A., and G. Oster. 1996. Cell motility driven by actin polymerization. *Biophys. J.* 71:3030–3045.
9. Kusumi, A., T. K. Fujiwara, …, K. G. N. Suzuki. 2012. Membrane mechanisms for signal transduction: the coupling of the meso-scale raft domains to membrane-skeleton-induced compartments and dynamic protein complexes. *Semin. Cell Dev. Biol.* 23:126–144.
10. Svitkina, T. 2007. Electron microscopic analysis of the leading edge in migrating cells. *Methods Cell Biol.* 79:295–319.
11. Chhabra, E. S., and H. N. Higgs. 2007. The many faces of actin: matching assembly factors with cellular structures. *Nat. Cell Biol.* 9:1110–1121.
12. Gittes, F., B. Mickey, …, J. Howard. 1993. Flexural rigidity of microtubules and actin filaments measured from thermal fluctuations in shape. *J. Cell Biol.* 120:923–934.
13. Brown, C. M., B. Hebert, …, P. W. Wiseman. 2006. Probing the integrin-actin linkage using high-resolution protein velocity mapping. *J. Cell Sci.* 119:5204–5214.
14. Yi, J., X. S. Wu, …, J. A. Hammer, 3rd. 2012. Actin retrograde flow and actomyosin II arc contraction drive receptor cluster dynamics at the immunological synapse in Jurkat T cells. *Mol. Biol. Cell.* 23:834–852.